Contents lists available at ScienceDirect

Plant Stress

journal homepage: www.sciencedirect.com/journal/plant-stress

Antagonistic manipulation of ER-protein quality control between biotrophic pathogenic fungi and host induced defense

Theoni Margaritopoulou [a,*], Konstantinos Kotsaridis [b], Martina Samiotaki [c], Spyridon Nastos [a], Marinos Maratos [a], Ieronymos Zoidakis [d,e], Despoina Tsiriva [f], Stergios Pispas [g], Emilia Markellou [a]

[a] *Laboratory of Mycology, Scientific Directorate of Phytopathology, Benaki Phytopathological Institute, Kifissia 14561, Greece*
[b] *Laboratory of Virology, Scientific Directorate of Phytopathology, Benaki Phytopathological Institute, Kifissia 14561, Greece*
[c] *Protein Chemistry Facility, Biomedical Sciences Research Center "Alexander Fleming", Vari, 166 72, Greece*
[d] *Department of Biology, National and Kapodistrian University of Athens, Panepistimioupolis, Zografou 15771, Greece*
[e] *Proteomics Laboratory, Biomedical Research Foundation, Academy of Athens, Athens 11527, Greece*
[f] *Research and Development Department, Phytorgan SA, Nea Kifissia, Greece*
[g] *Theoretical & Physical Chemistry Institute, National Hellenic Research Foundation, Athens 11635, Greece*

ARTICLE INFO

ABSTRACT

The interaction of plants with pathogens during infection is a multifaceted process involving various molecules deriving from both partners. A current goal in combating pathogen virulence is to induce plant resistance using environmentally friendly compounds. Here, we show that chitosan-based nanoparticles loaded with the defense hormone salicylic acid, can efficiently activate defense responses and reactive oxygen species (ROS) production and *PATHOGENESIS RELATED-1* (*PR1*) expression in *Arabidopsis thaliana* leaves, and reduce conidial germination of the biotrophic pathogenic fungus *Podosphaera xanthii*. Transcriptomic and proteomic analyses identified immune response-related upregulated transcripts and proteins after nanoparticle application, highlighting the Leucine Rich Repeat (LRR)-, Systemic Acquired Resistance (SAR)-, and glutathione-related protein groups. Examination of *P. xanthii* during infection at control conditions, identified ribosomal, hydrolase-related, putative secreted and effector proteins, while nanoparticle application significantly downregulated their expression. An in-depth investigation of the highly expressed proteins in *P. xanthii* and Arabidopsis revealed the involvement of components of endoplasmic reticulum protein quality control (ERQC) in the pathogen-host interaction. The RPS27A effector protein was identified in fungal virulence, while endoplasmic reticulum (ER) protein processing- and glycosyltransferase-related proteins were implicated in plant's induced defense response following nanoparticle application. Overall, these findings demonstrate that the ERQC is dynamically manipulated by both the pathogen for efficient virulence and by elicitors for plant induced defense.

1. Introduction

Biotrophic plant pathogenic fungi constitute some of the most destructive pathogens that can cause major losses of agriculturally important crops (Gan et al., 2011). The successful lifestyle of these pathogens depends on the establishment of a dynamic relationship with living plant cells through which they hijack plant resources to support pathogen growth and reproduction (Kemen et al., 2015). The interaction of biotrophs with their plant hosts is finely tuned during evolution. This communication allows pathogens to escape the pressure of plant's

defense responses and to transfer nutrients from the host cell, an aggressive interplay between pathogen virulence and host resistance (Kemen et al., 2015).

The pursuit of productivity, due to the rapid growth of the world's population, forced the abuse of fertilizers and pesticides, to prevent devastating losses because of plant diseases, that inevitably caused serious environmental pollution and ecological damage (Chu and Karr, 2017). Consequently, the main concerns in the agricultural industry have changed from improving crop yield to sustaining food quality and reducing environmental impact, that led to the need of environmentally

---

friendly agricultural inputs (Bremmer et al., 2021). A very prominent way to achieve this is by empowering plants to withstand pathogen attack with the use of resistance inducers, compounds that increase the level of plants basal resistance against future attacks compared to non-stimulated plants (Reglinski et al., 2023). Chitosan is a well-known bio-stimulant used for promotion of growth and induction of resistance (Faqir et al., 2021). Chitosan nanoparticles (CNPs) can act as growth enhancers and potent antimicrobial agents against pathogenic fungi and as biodegradable materials can be explored in various fields in their nano form to replace non-biodegradable and toxic compounds (Ingle et al., 2022). Additionally, CNPs can also act as a delivery matrix for various compounds of interest, providing steady and slow release of these compounds (Sembada and Lenggoro, 2024). CNPs have mainly been studied for biomedical applications (Bashir et al., 2022). Recently, evidence have shown that CNPs, empty or loaded with Cu, can induce defense activity of plants against phytopathogens (Ingle et al., 2022). Salicylic acid (SA) is a key defense hormone synthesized by plants upon attack by biotrophic pathogens and the endogenous signal responsible for inducing systemic acquired resistance (SAR) (Gaffney et al., 1993). SA can be monitored by *PR1* gene, an essential component of plant's defense mechanism, and a major SAR response marker against biotrophic pathogens (Van Loon and Van Strien, 1999).

SA in high doses can act as an antagonist and have a negative rebound effect of inhibition in plant growth and development. To maintain optimal SA concentrations in the long term, it is necessary to develop systems that deliver and slowly release SA in plants. To ensure the optimal outcome in improving plant defense by SA, its delivery and release should be controlled, since high doses can be antagonistic with negative effects on plant growth and development (Polyakov et al., 2023). Synthesis of CNPs loaded with SA can achieve this goal and be highly productive in inducing plant defense.

Once the pathogen has penetrated the external barriers of the host, like waxy cuticles and the cell wall, it encounters the first level of the plant defense system on the plant cell membrane: pattern recognition receptors (PRRs), such as leucine-rich repeat receptor kinases (LRR-RKs), identify the pathogen associated molecular patterns (PAMPs) and trigger PAMP-immunity (PTI) (DeFalco and Zipfel, 2021; Dodds and Rathjen, 2010). At this level of plant defense, various cellular components of the pathogen get detected by host machinery leading to an immune response against the pathogen. To bypass PTI, the pathogen also responds by secreting a set of specialized proteins called effectors, usually small-sized proteins with <300 amino acids, that have unique actions in manipulating the host machinery. In response to PTI, numerous strategies have been used by the pathogen with the help of its effectors to surpass the PTI system and compromise the host immunity. This initiates the second level of plant immune defense, Effector-triggered immunity (ETI), in which plant nucleotide-binding leucine-rich repeat proteins (NLRs), that are nucleotide-biding proteins, recognize the secreted effectors (Dodds and Rathjen, 2010). ETI is a more robust, specific, and indispensable defense system that comes into play and takes over the defense pathways with prolonged effectiveness compared to PTI (Jaswal et al., 2020). Although PTI and ETI are of two different levels of the plant immune system, both share numerous genes and pathways of the immune signaling network (Pruitt et al., 2021; Tian et al., 2021; Yuan et al., 2021). PTI and ETI activation share many signals and components leading to the downstream effects of activation of the mitogen-activated protein kinases (MAPK) pathways, stomatal closure, transcriptional reprogramming of defense responsive genes, pathogenicity related (PR) genes, hypersensitive response, reactive oxygen species (ROS) burst and callose (Margaritopoulou et al., 2022; Stael et al., 2015).

Component manipulation of the defense pathways of the host is probably the principal function that biotrophic fungal effectors are known to be involved in Nevertheless, the molecular mechanisms underlying this effector-mediated manipulation of host defense pathways are mainly unknown, even though there have been attempts to

functionally characterize the effectors (Jaswal et al., 2020). Over-expression experiments of effectors proteins in alternate hosts or heterologous systems resulted in identifying networks that influence pathogen effectors and modulate plant immunity. The nodes of these networks are suggested to be composed of interactions between numerous underlying pathways, such as hypersensitive-induced cell death, suppression of programmed cell death (PCD) pathway, ROS accumulation, and leakage of essential electrolytes (Ahmed et al., 2018). The main events modulated by the interchanged nodes are suppression of PTI, modification of the host transcriptional and post-transcriptional processes, targeting of various organellar processes, and hijacking the host metabolism especially for reducing the levels of the SA defense hormone (Jaswal et al., 2020).

Here, we present a study in which a combination of physiological, histochemical, transcriptomic and proteomic approaches was used to elucidate the molecular mechanisms underlying the action of chitosan nanoparticles, loaded with SA, as an inducer of resistance in *A. thaliana*, and the response of the biotrophic pathogen *P. xanthii*. The efficiency of this novel delivery system for plant disease control, that can also act as a potential growth stimulator, was evaluated through the analysis of parameters related to root growth, pathogen germination and induction of *PR1* resistance-marker gene and ROS generation. At the molecular level, we assessed both the host and pathogen's responses revealing that key functional pathways related to protein synthesis, protein quality control and degradation are selectively employed by the host to induce defense, after SA-CNPs application and by the pathogen effectors to disrupt host defenses and promote infection. Biodegradable nanoparticles can be significantly associated with strategies for nanoscale application of active ingredient and slow release, and this work sheds light on their mode of action, particularly within the context of host-pathogen interaction.

2. Materials and methods

2.1. Plant material and growth conditions

A. thaliana Col-0 (wild-type) and *PR1::GUS* (N6357) seeds were obtained from the Arabidopsis Stock Center and used in the experiments. The seeds were sterilized for 20 s in 70 % ethanol, followed by 1.5 min in 20 % bleach solution, and rinsed five times with sterile water. The seeds were sown on half-strength Murashige and Skoog (MS) medium with 1 % sucrose and 0.7 % agar, stratified at 4 °C in the dark for 2 days, and transferred to a 23 °C growth chamber under long day (16 h light/8 h dark) conditions.

2.2. Preparation and characterization of chitosan nanoparticles

Chitosan nanoparticles loaded with SA (SA-CNPs) were synthesized using the ionic gelation method, resulting in final nanoformulations based on NanoShield technology. Industrial-grade chitosan hydrochloride (molecular weight 61 kDa, degree of deacetylation 85 %) and industrial-grade salicylic acid were employed for the formulation. Chitosan was dissolved in 1 % acetic acid solution and vigorously stirred until the solution became clear. The chitosan solution was set on a magnetic stir and aqueous anionic cross linker was added dropwise. The mixture was homogenized prior to purification and collection.

The physicochemical characterization of the CSNPs/SA nano-formulation was carried out at National Hellenic Research Foundation, Theoretical and Physical Chemistry Institute (NHRF/TPCI). The produced CSNPs/SA were studied using Dynamic Light Scattering (DLS) to determine the hydrodynamic radius/size (Rh), the polydispersity index (PDI), and the scattered light intensity (Intensity) from the nanoparticle solution (a parameter related to the mass of the nanoparticles formed each time). Measurements of the synthesized CS-NPs/SA were performed 24 h after their preparation at 45°, 90°, and 135° scattering angles at a temperature of 25 °C. The analysis of the autocorrelation

functions from DLS was conducted using the cumulants method and the CONTIN algorithm. The experiments were conducted using the available wide-angle light scattering photometer of NHRF/ TPCI (CGS-3, ALV GmbH).

2.3. Chitosan nanoparticles application

A. thaliana Col-0 (wild-type) and *PR1::GUS* (N6357) seeds were grown for 5 days in half-strength MS medium petri dishes and then transferred to half-strength MS medium square plates supplemented with different concentrations (5, 10, 20, 40 and 100 ppm) of SA-CNPs.

2.4. Pathogen challenge accompanied by hormone treatment

Pathogen artificial inoculation was performed with a 5μl high pressure spore suspension (10^7 spore/ml) of *P. xanthii*. The spore suspension was dropped onto the leaves of 12-D-old Arabidopsis plants grown on half-strength MS medium square plates supplemented with and without 5 ppm SA-CNPs. All inoculated plants were incubated at 22 °C with a 16-h light:8-h dark photoperiod and 65 % relative humidity. For molecular analyses, treated and non-treated 14-D-old plants, with root excision, were collected in liquid nitrogen and stored in −80 °C until use.

2.5. Root growth analysis

For growth comparison, Arabidopsis Col-0 and *PR1::GUS* 5d plants were transferred to half-strength MS medium square plates supplemented with the tested SA-CNPs concentrations. Primary root length was recorded each day by measuring from root tip to hypocotyl base with ImageJ software (http://rsbweb.nih.gov/ij/). All data are mean values of at least 20 plants, and the experiments were repeated three times. Statistical analysis was performed with Prism ver.10 (GraphPad, USA).

2.6. Microscopy

To examine conidial germination, leaves were stained with Calcofluor white stain (Fluka, Switzerland) and microscopic observations were carried out. 300 conidia were measured for each treatment and genotype.

Detailed observation of *P. xanthii* conidia was performed by an SP8 confocal microscope (Leica, Germany). Conidia were visualized with the chitin-binding wheat germ agglutinin (WGA) conjugated with the fluorescent dye CF-488 (Biotium, USA). Excitation was performed with the 488 nm line of the White Light Laser (WLL) and emission filtering was achieved using a 510- to 540-nm bandpass filter. During image acquisition each line was scanned 6 times and averaged. Image processing was performed using functions of the LAS X (Leica, Germany) operating software.

2.7. Histochemical analyses

For in situ accumulation of ROS, hydrogen peroxide (H_2O_2) and superoxide radical (O_2^-) were assessed. H_2O_2 was determined according to the 3, 3′-diaminobenzidine (DAB)-uptake method. 12-day old Arabidopsis plants, after 7 days in MS plates supplemented with 5 ppm SA-CNPs, were incubated in 0.1 % DAB (pH 3.8) for 2 h in plates covered with aluminum foil at room temperature (25 °C), and then were treated with boiling ethanol at 95 °C to stop the reaction and bleach the plants. Examination was performed under stereoscope for brownish precipitates that correspond to H_2O_2 accumulation.

The nitroblue tetrazolium (NBT) (N6876, Sigma-Aldrich) staining method was used for the detection of O_2^-. Arabidopsis plants, with same treatment as in DAB staining, were immersed in 3.5 mg ml^{-1} NBT staining solution in potassium phosphate buffer (10 mM). Stained plantlets were bleached as in DAB staining procedure. O_2^- was visualized as a blue color produced by NBT precipitation.

2.8. GUS assays

Plants of Arabidopsis were used for SA-CNPs treatment and/or pathogen inoculation. Plants were immersed in staining solution (100 mM NaPO₄ [pH 7.0], 0.5 mM K₃Fe(CN)₆, 0.5 mM K₄Fe(CN)₆, 10 mM EDTA, 0.1 % [v/v] Triton X-100, 1 mM 5-bromo-4-chloro-3-indolyl-b-D-glucuronic acid substrate in DMSO [diluted from a 25 mM stock solution]) as described by (Jefferson et al., 1987). After staining at 37 °C for 30 min in the dark, samples were rinsed and fixed in 75 % ethanol.

2.9. RNAseq and data analysis

RNA samples were isolated using NucleoSpin RNA Plant and Fungi (Macherey Nagel, Düren, Germany) following the manufacturer's instructions. The RNA-seq libraries were generated using the Illumina TruSeq RNA sample preparation kit and sequenced on an Illumina NovaSeq 6000 system via paired-end sequencing to obtain 101 bp single end reads. The reads were mapped to the *A. thaliana* reference genome version TAIR10 (accession: GCA_000001735) using STAR version 2.5.3. a54 (Dobin et al., 2013). Expression counts were generated using the R function summarize Overlaps from the package HTSeq (Anders et al., 2015) in union mode on exons. Differential expression analyses were performed using the R package DESeq version 1.32.055 (Anders, 2010). Differentially expressed were considered genes with absolute log2-FoldChange ±1. GO enrichment analysis of DEGs was performed using Cytoscape (Shannon et al., 2003). For *P. xanthii*, the reads were mapped to the complete genome sequence of *P. xanthii* isolate YZU573 (Wang et al., 2023) using Kallisto software (Bray et al., 2016). Secreted and effector protein analysis was performed by combining the two published *P. xanthii* effector databases (Kim et al., 2021; Wang et al., 2023).

2.10. Protein extraction, digestion, and identification

Arabidopsis samples were homogenized and lysis buffer (4 % SDS, 0.1 M DTT, 0.1 M Tris pH 7.4) was added. The samples were heated for 3 min at 99 °C followed by centrifuge at 17000x*g* for 15 min. The lysed samples were processed according to the Sp3 protocol (Hughes et al., 2019) including an alkylation step in 200 mM iodoacetamide (Acros Organics). 20 μg of beads (1:1 mixture of hydrophilic and hydrophobic SeraMag carboxylate-modified beads, GE Life Sciences) were added to each sample in 50 % ethanol. A magnetic rack was used for protein clean-up. The beads were washed two times with 80 % ethanol and once with 100 % acetonitrile (Fisher Chemical). The captured-on beads proteins were digested overnight at 37 °C under vigorous shaking (1200 rpm, Eppendorf Thermomixer) with 1 μg Trypsin/LysC (MS grade, Promega) prepared in 25 mM ammonium bicarbonate. Next day, the supernatants were collected, and the peptides were purified using a modified Sp3 clean up protocol and finally solubilized in the mobile phase A (Buffer A: water with 0.1 % formic acid). After sonication, a nanodrop instrument was used for determining peptide concentration at 280 nm absorbance.

Samples were run on a liquid chromatography tandem mass spectrometry (LC-MS/MS) setup consisting of a Dionex Ultimate 3000RSLC online with a Thermo Q Exactive™ HF-X Orbitrap mass spectrometer (Thermo Fisher Scientific Inc., Waltham, MA, USA). The peptidic samples were directly injected and separated on a 25 cm-long analytical C18 column (PepSep, 1.9μm3 beads, 75 μm ID, Bruker) and ionized trough a pepsep sprayer equipped with a liquid junction stainless steel emitter using a one-hour long run, starting with a gradient consisting of 7 % Buffer B (0.1 % Formic acid in 80 % Acetonitrile) to 35 % for 40 min and followed by an increase to 45 % in 5 min and a second increase to 99 % in 0.5 min and then kept constant for equilibration for 14.5 min. Sample loading phase had a 400 nL/min flow rate, while it lowered to 250 nL/min in main phase of sample analysis. A full MS was acquired in profile

and positive mode using a mass spectrometer, operating in the scan range of 375–1400 *m/z* using 120 K resolving power with an AGC of 3×106 and max IT of 60 ms followed by data independent analysis using 8 Th windows (39 loop counts) with 15 K resolving power with an AGC of 3×105 and max IT of 22 ms and a normalized collision energy (NCE) of 26.

Orbitrap raw data was analyzed in DIA-NN 1.8.1 (Data-Independent Acquisition by Neural Networks) (Demichev et al., 2020) through searching against the reference proteomes of Arabidopsis (UP000006548_3702) retrieved from Uniprot database and *P. xanthii* isolate YZU573, in the library free mode of the software, allowing up to two tryptic missed cleavages. The DIA runs created a spectral library

that was used for re-analysis. DIA-NN at default settings were used with addition of the variable modifications of oxidation of methionine residues and acetylation of protein N-termini, and the carbamidomethylation of cysteine residues as fixed modification. N-terminal methionine excision was also enabled. The match between runs (MBR) feature was used for all analyses and the output (precursor) was filtered at 0.01 FDR and finally the protein inference was performed on the level of genes using only proteotypic peptides.

The generated results were processed statistically and visualized in the Perseus software (1.6.15.0) (Tyanova et al., 2016). Values were log (2) transformed, a threshold of 70 % of valid values in at least one group was applied and the missing values were replaced from normal
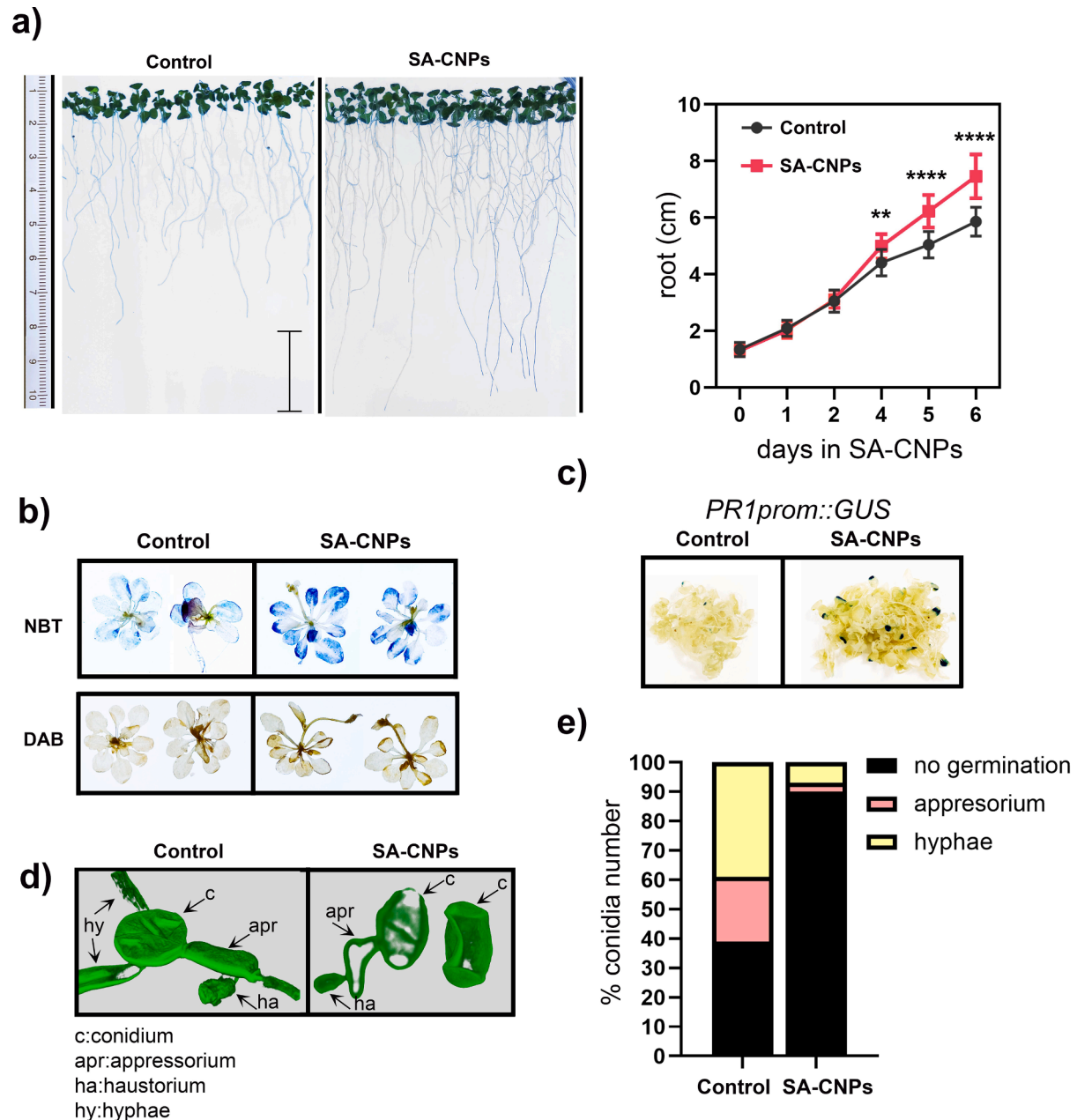
Fig. 1. SA-CNPs positively regulate defense responses against *P. xanthii*. **(a)** *A.thaliana* plants are more developed with longer roots in media supplemented with SA-CNPs than in the Control. 5-ᴅ-old seedlings were transferred from Control media to SA-supplemented media for 7 days. Bar indicates the increase in root length. Values are means ± SEs ($n \geq 20$) (**$P < 0.01$ and ****$P < 0.0001$; Student's *t*-test). **(b)** Representative images of 3,3'-diaminobenzidine (DAB) and nitroblue tetrazolium (NBT) staining of *A.thaliana* plants grown either in Control media or in media supplemented with 5 ppm SA-CNPs. **(c)** Gus staining of 5 *PR1::GUS* transgenic plants grown either in Control media or in media supplemented with 5 ppm SA-CNPs. **(d)** 3D images obtained using confocal microscopy and showing delayed growth of *P. xanthii* conidia on leaves of *A.thaliana* plants grown in media supplemented with 5 ppm SA-CNPs compared to Control. Images were taken at 40 hpi. **(e)** Quantification of germinated *P. xanthii* conidia and the development of fungal structures at 40 hpi.

distribution. For statistical analysis, Student's *t*-test was performed, and permutation-based FDR was calculated.

2.11. Protein tertiary structure predictions and comparisons software

The 3-dimensional (3D) conformations of the investigated proteins were forecasted using the AI-based Alphafold2 online server (Jumper et al., 2021). Following this, comparisons between the tertiary protein structures and those available in the Protein Data Bank (PDB) (Berman et al., 2003) were conducted utilizing the Dali server (Holm, 2020). Visualization of the 3D structural representations of the protein molecules was accomplished using Pymol software (Schrödinger and DeLano, 2020).

3. Results

3.1. SA-CNPs application upregulates defense responses against the biotrophic pathogen P. xanthii

To study the effectiveness of CNPs in inducing Arabidopsis defense against *P. xanthii*, we synthesized CNPs loaded with Salicylic acid (SA-CNPs). Nanoparticle tracking analysis revealed that the produced SA-CNPs had an average particle size distribution of 167 nm (Fig. S1), which complies with the European Food Safety Authority (EFSA) risk assessment guidelines of nanomaterial application (Committee, 2021). Before performing the induction of defense experiment against *P. xanthii* infection, the synthesized SA-CNPs were tested for phytotoxicity on Arabidopsis seedlings at concentrations ranging from 5 to 100 ppm. The results showed that increased dose was inversely correlated with seedling root growth, except at the 5 ppm dose, where SA-SCPs significantly enhanced Arabidopsis root and overall plant growth (Fig. 1A, Fig. S2A-2E, *p-value* < 0.0001). This is consistent with the growth
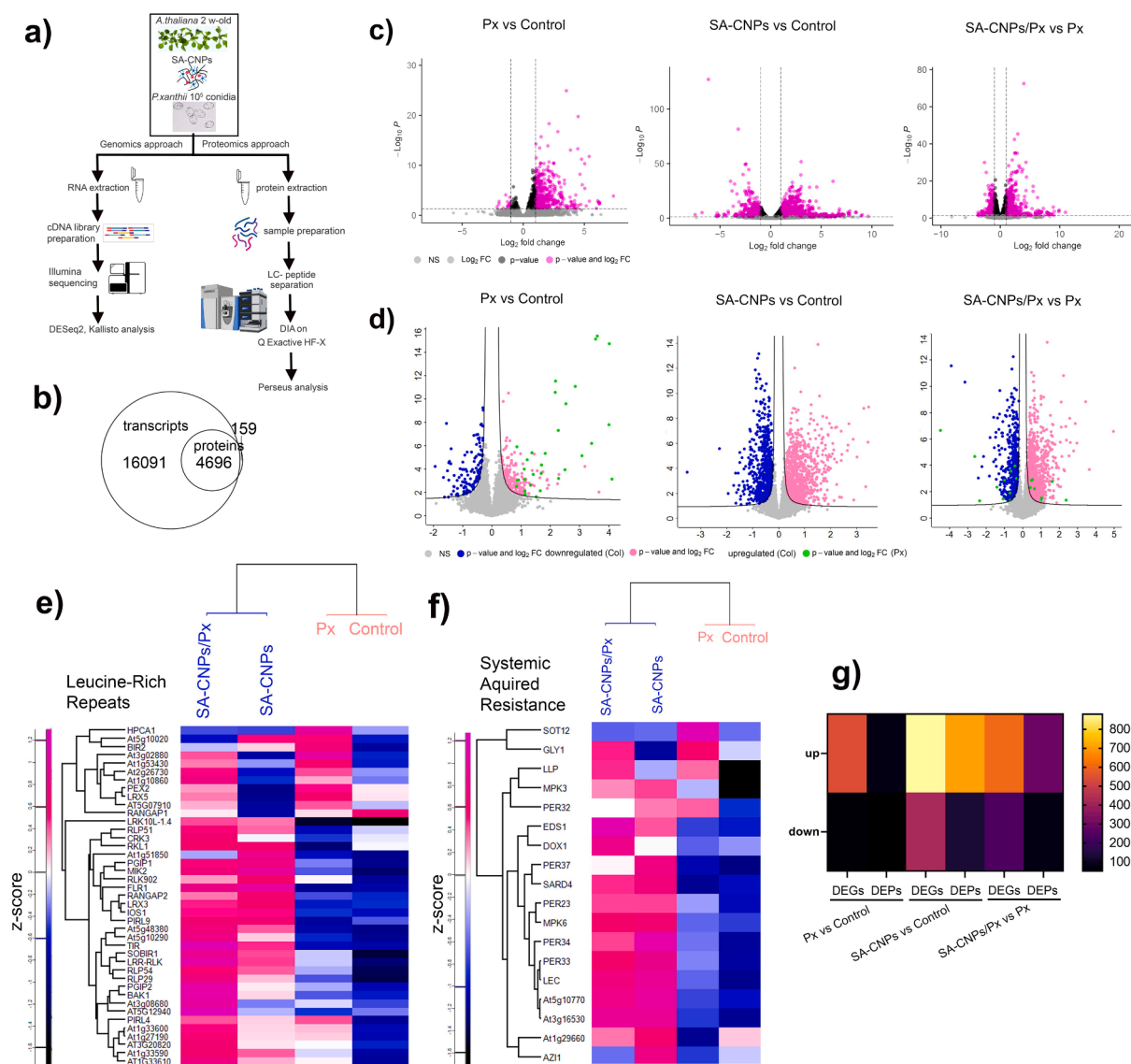
Fig. 2. Upregulation of transcript and protein abundance after SA-CNPs application. **(a)** Schematic representation of the RNAseq and proteomic workflows. **(b)** Overlap of *A.thaliana* total genes and proteins in the integrated transcriptomic and proteomic analysis. **(c,d)** Volcano plots showing the positive and negative differential expressed genes (**C**) and proteins (**D**). **(e, f)** Upregulation of key defense sensors and responses by SA-CNPs. Heatmaps of differentially expressed proteins that are related to leucine-reach repeats structural motifs (**E**) and to systemic acquired resistance mechanism (**F**) in *A. thaliana* leaves. **(g)** Abundance of upregulated and downregulated transcripts and proteins in the significant comparisons of the treatments.

promoting effects of low SA concentrations mediated by SA- control over cell division and expansion (Li et al., 2022). Additionally, testing empty CNPs or free SA at the concentration of 5 ppm each showed either moderate or substantial inhibition of root growth development, respectively (Fig. S2F, S2 G). At 5 ppm, SA-CNPs demonstrated significant potential to increased ROS accumulation, as shown by DAB and NBT staining, and by upregulating *PATHOGENESIS-RELATED PROTEIN 1* (*PR1*) gene expression in the *PR1::GUS* transgenic line, indicating substantial induction of defense responses in Arabidopsis (Fig. 1B, 1C).

To test the efficacy of the synthesized SA-CNPs against *P. xanthii*, Arabidopsis seedlings were artificially inoculated with a high-pressure conidial suspension. Confocal microscopy, 40 h post inoculation, revealed considerable differences in conidial germination between treatments. In untreated control plants >50 % of the conidia had germinated and at least one out of three had developed hyphae structures. In contrast, in SA-CNPs treated plants germination was significantly decreased by 70 % (Fig. 1D, 1E, S3, *P-value* = 0.0362). This result highlights the high potential of SA-CNPs as elicitors of defense mechanisms, especially given that the nanoparticles were incorporated into the growth medium without direct contact with *P. xanthii* conidia.

3.2. Transcriptional and proteomic changes after SA-CNPs application and pathogen inoculation in Arabidopsis

The molecular pathways underlying the induction of defense mechanisms by SA-CNPs, were investigated by a combined transcriptomics and proteomics approach (Fig. 2A). Arabidopsis 14-D-old plants treated and untreated with 5 ppm SA-CNPs, before and after pathogen inoculation were used for omics analyses. A total of 20,787 transcripts and 4855 proteins were detected in our datasets (File S1). The principal-component analysis (PCA) plot for each data set showed that plant samples were grouped according to treatment (Fig. S4). Additionally, 97 % of the identified proteins overlapped with 29.2 % of the identified Arabidopsis gene transcripts, indicating a satisfactory representation of the Arabidopsis gene pool in our data sets (Fig. 2B). To analyze the relationship between inducer application and pathogen inoculation, expression comparisons were made at the transcriptome and at the proteome level. SA-CNPs application significantly influenced the expression of 3745 genes and 2368 proteins, and both SA-CNPs application and pathogen inoculation changed the expression of 3540 genes and 1309 proteins, when compared to pathogen inoculated plants (SA-CNPs*P. xanthii* vs *P. xanthii* comparison) (File S1). On the other hand, pathogen inoculation changed the expression of fewer genes; specifically, 1689 transcripts and 289 proteins were detected, indicating a constricted effect on Arabidopsis responsive pathways (Fig. 2C, 2D, File S1). When the protein data sets were matched against the database of the *P. xanthii* protein annotation, 35 proteins of the fungus were identified in the inoculated samples that were decreased to 14 proteins in the SA-CNPs and pathogen treated samples (Fig. 2D, Tab. S1). Heatmaps for both transcriptomic and proteomic results revealed clustering between SA-CNPs treated and untreated Arabidopsis samples and the differences among these treatments were highly apparent at the proteome level (Fig. S5).

Evaluation of the proteomic profiles for specific protein functions revealed notable results. SA-CNPs application positively influenced the expression of 30 out of the 41 detected LRR-RKs (Fig. 2E). Moreover, when we searched for SAR-related proteins we detected 17 associated proteins that included the well-known pathogen-responsive MPK3 and MPK6 kinases, 5 ROS-related peroxiredoxins, and EDS1, an essential component of R gene-mediated disease resistance (Beckers et al., 2009; Falk et al., 1999; Survila et al., 2016) (Fig. 2F).

To get a more detailed perception of the SA-CNPs effects, we narrowed down the identified gene and protein pool to the highly differentiated ones by setting the cut off to 1 log2fold change for transcripts and 0.8 log2fold change for proteins. Even though the comparisons between treatments did not change, the analysis revealed that the

inducer primarily upregulates gene expressions, while downregulation takes place to a limited extent (Fig. 2G, File S2). For example, SA-CNPs application positively changes the expression of 705 Arabidopsis proteins, while only 131 proteins are negatively regulated. As expected, *PR1* expression was remarkably upregulated both in transcript with Log2FC = 5,3 and in protein with Log2FC = 4.2, (File S2).

3.3. Comprehensive functional annotation of the upregulated genes

To elucidate the potential functions of the genes involved in the induction process, we examine the Gene Ontology (GO) classifications of all differentially expressed gene transcripts and proteins identified in Arabidopsis were examined, filtered by log2fold cut-off. Notably, no significant functional enrichment was observed in any of the downregulated groups, either transcripts or proteins, indicating a moderate negative effect of the inducer or pathogen on Arabidopsis genetic networks (File S3). On the contrary, various significant functional enrichments were found in the upregulated groups. Analysis of overlapping GOs in the transcript groups yielded noteworthy results (Fig. 3A, File S3). In the pathogen inoculation vs control (*P. xanthii* vs C) comparison, 91 terms-representing the 87.5 % of the enriched GO terms- were shared with 45.9 % of the terms in the SA-CNPs application vs control comparison (SA-CNPs vs C). This suggests a substantial link between elicitation and pathogen infection, with elicitation mimicking pathogen infection, through shared genetic networks.

The *P. xanthii* vs C treatment yielded no significant differentially expressed proteins, which may reflect a moderate response of Arabidopsis at this early stage of infection. The overlap of enriched GO terms in both transcripts and proteins groups from the SA-CNPs vs C comparison showed that SA-CNPs application made directed changes in plant responses, as 33 % of the enriched GO terms in the protein group were also found in the transcript group. In contrast, when combined with pathogen inoculation in SA-CNPs/*P. xanthii* vs *P. xanthii* comparison, the shared GO terms dropped to 22 %, suggesting a higher differentiation in the plant's genetic networks (Fig. 3B, File S3). Since SA-CNPs vs C comparisons represent a typical induced defense response, we selected the overlapping groups of transcripts and proteins of this comparison for further analysis. A substantially number of genes participated in the 18 enriched GO terms which are defense related, such as "plant-pathogen interaction", "systemic acquired resistance", "cell wall", "response to reactive oxygen species", "secretory vesicle", "glutathione transferase activity" and "programmed cell death" (Fig. 3C, File S4). Among these, 7 GO terms were also present to the SA-CNPs/*P. xanthii* vs *P. xanthii* protein groups comparison, suggesting a stronger link to defense mechanisms. Four additional GO terms were shared between both protein groups, and these were analyzed further. These enrichments were associated with systemic acquired resistance, glutathione activity, toxin metabolism, chitinases, secretion and quercetin 3-O-glycosyltransferase activity, a flavonol that induces salicylic acid biosynthesis (An et al., 2023) (Fig. 3D). The 38 proteins that comprised these terms were subjected to STRING analysis that 27 (71 %) formed a functionally associated network with a highly significant Protein-Protein Interaction (PPI) enrichment (*P-value*: < 1.0e-16). (Fig. 3E). Among the interacting proteins, eight glutathione S-transferases involved in detoxification (GSTs; (Gullner et al., 2018)), two glycosyltransferases involved in glycoside biosynthesis (UGTs; (Gharabli et al., 2023)), a class I PR4 vacuolar protein with strong antifungal activity (HEL/PR4; (Bertini et al., 2012)), a mitogen-activated protein kinase involved in induced defense response (MPK3; (Beckers et al., 2009)), a chitinase that inhibits fungal growth (CHI; (Vaghela et al., 2022)) and a glucan endo-1,3-beta-glucosidase (BGL2/BG2) which defense responses by balancing callose production (Liu et al., 2024) (Fig. 3D, 3E). Furthermore, HEL was shown to interact with 10 proteins of our network. Further analysis of the HEL protein sequence using SignalP (v5.0) identified a signal peptide at amino acids 1–20, with a cleavage probability of 0.847077 at glycine-21, directing the protein
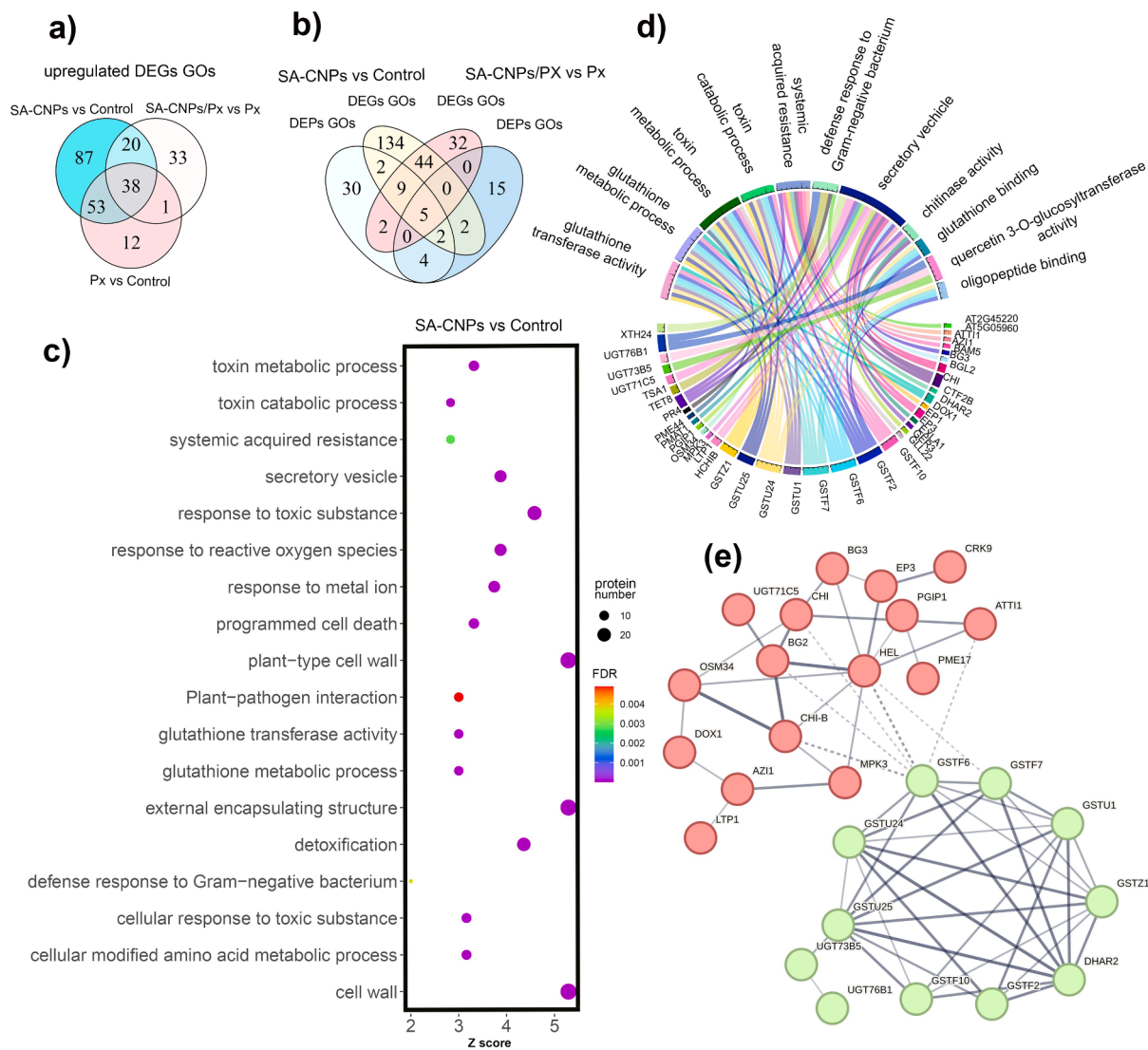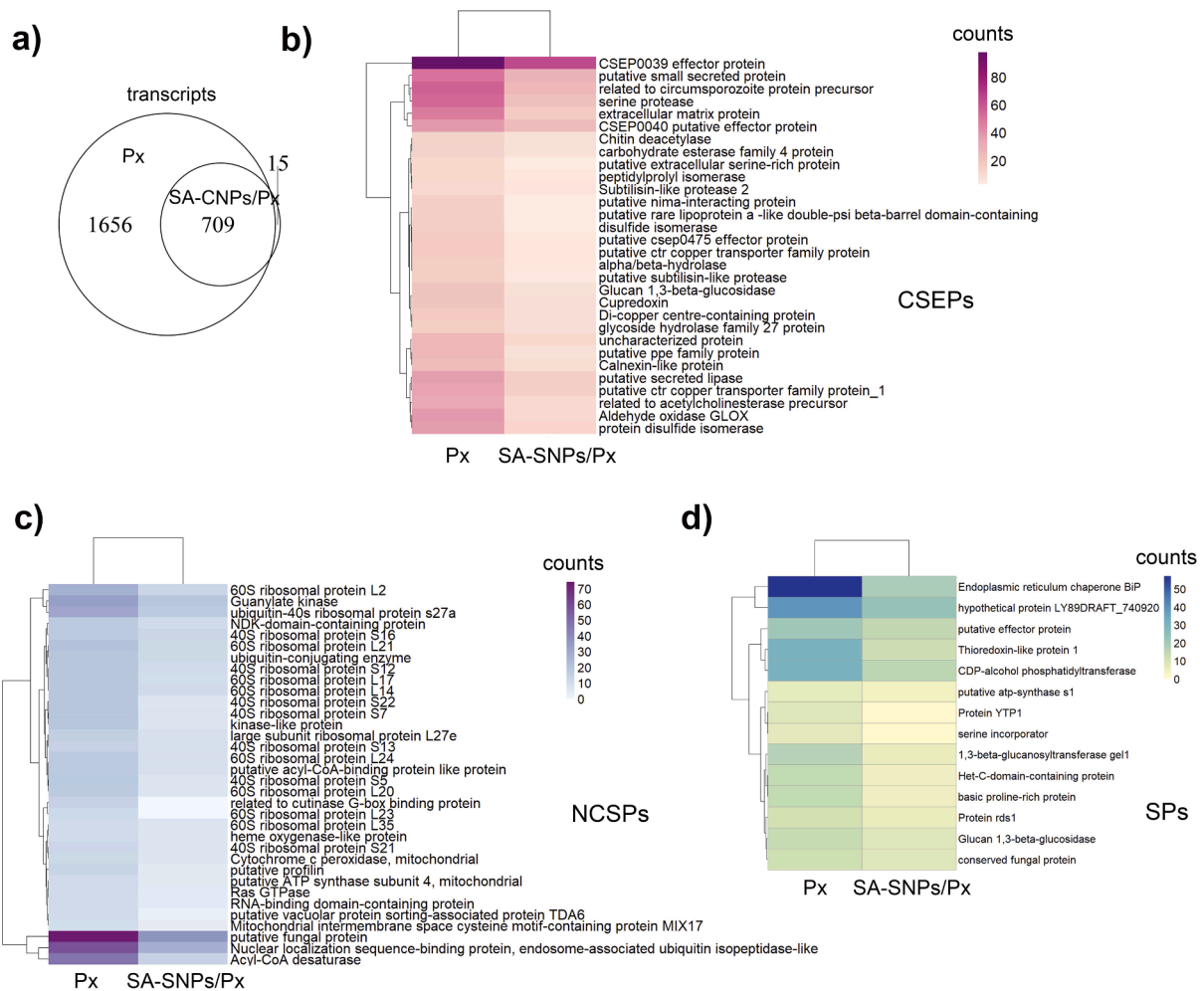
Fig. 3. Characterization of defense pathways and proteins after SA-CNPs application. **(a)** Overlap of *A.thaliana* differentially expressed genes in the statistically significant treatments. **(b)** Overlap of *A.thaliana* differentially expressed genes and proteins in the integrated transcriptomic and proteomic analysis. **(c)** Pathway enrichment analysis of differentially expressed proteins identified in the SA-CNPs vs Control comparison. **(d)** Circos plot showing eleven identified important enriched pathways after SA-CNPs application. The pathways are comprised of defense-related genes corresponding to GSTs, HEL/PR4, MPK3, and CHI among others. The lines represent the association of enriched pathways with the matching genes. **(e)** PPI network of the identified proteins in the important enriched pathways after SA-CNPs application.

toward the secretory pathway (Fig. S6). Overall, the results suggest that SA-CNPs enhance the production of an integrated defense network comprising GST activation, protein glycosylation, chitin degradation and secretion, all of which are key responses to fungal pathogen infection.

3.4. Downregulated expression of P. xanthii effectors after SA-CNPs application

The in-depth investigation of Arabidopsis molecular responses, coupled with the significant inhibition of *P. xanthii* conidial germination, following SA-CNPs application, raised the key question of what changes occur in the genetic pathways of the fungus. Transcriptome analysis of the fungus using Kallisto software quantified 2365 transcripts in the control samples and 724 transcripts in the SA-CNPs treated samples, with 709 shared between both treatments (Fig. 4A). We identified 78 transcripts of secreted proteins in our samples were categorized in three categories (Kim et al., 2021) (Fig. 4, Tab. S2). The first category consisted of 30 candidate secreted effector proteins (CSEPs) that were

mainly proteases, isomerases, hydrolases, and other enzymes targeting proteolytic degradation pathways (Fig. 4B). This aligns with increasing evidence that microbial effectors leverage the ubiquitin–proteasome system (UPS) as central hub in order to achieve global perturbation of the host cell (Langin et al., 2020). The second category was comprised of 34 non-classical secreted proteins (NCSPs) that were mainly ribosomal proteins (47 %), but there were also ubiquitin molecules, kinases and mitochondrial proteins (Fig. 4C). The third category was comprised of 14 secreted proteins (SPs) with most of them being membrane proteins such as an endoplasmic reticulum chaperone, a CDP-alcohol phospha-tidyl-transferase involved in phospholipid biosynthesis (Nogly et al., 2014), an integral mitochondrial membrane protein (YEAST PUTATIVE TRANSMEMBRANE PROTEIN 1, YTP1) and two glucan-related proteins. Interestingly, a thioredoxin-like (TRX-like) transcript was identified, corresponding to the TRX protein with cytoprotective role against various oxidative stresses (Lee et al., 2013) (Fig. 4D). The common feature between all the identified effector transcripts was that after SA-CNPs application, a noteworthy global reduction in their expression was observed (Fig. 4 and Table S3). So, it is obvious that the overall

Fig. 4. SA-CNPs application negatively influences *P. xanthii* secreted proteins expression. **(a)** Overlap of *P. xanthii* differentially expressed genes in the statistically significant treatments. **(b)** Heatmap showing reduced expression levels of the identified *P. xanthii* secreted effector proteins (CESPs) after SA-CNPs application. **(c)** Heatmap showing reduced expression levels of the identified *P. xanthii* non-classical secreted proteins (NCSPs) after SA-CNPs application. **(d)** Heatmap showing reduced expression levels of the identified *P. xanthii* secreted proteins (SPs) after SA-CNPs application.

downregulation of the fungal secretome reflects the reduced conidia germination after SA-CNPs application, demonstrating an essential suppression of fungal virulence by the plant.

3.5. The ubiquitin system is involved in fungal virulence and is depressed by induced defense

To further investigate the effect of host induced defense on fungal virulence, we examined the pathogen at the proteome level. We identified 34 proteins in the *P. xanthii* samples and 15 proteins in the SA-CNPs/*P. xanthii* samples, with 10 of them being common between the treatments (Fig. 5A, Table S4). Almost all the identified fungal proteins (88 %) in the *P. xanthii* samples were also detected as transcripts, while in the SA-CNPs/*P. xanthii* samples the percentage decreased to 60 % (Fig. 5A). The divergence in protein and transcript pools in the SA-CNPs/*P. xanthii* samples was similar to what we noticed in Arabidopsis protein to transcript correlations (Fig. 3B), indicating that diverse levels of regulation between transcripts and proteins were also present inside the pathogen (Fig. 5A).

Inside the protein pool of the pathogen, at non-treated conditions, we identified six secreted proteins (Tab. S5). Four of the secreted proteins were NCSPs and were characterized, by the database that we used for protein identification, as a ubiquitin-40S ribosomal protein s27a (RSP27A), a nuclear localization sequence-binding protein (NL-SBP), a large subunit ribosomal protein L27e (RPL27) and a putative fungal

protein (PFP). The other two proteins belonged to the SP category and were characterized as a ribosome-recycling protein (RRF) and an endoplasmic reticulum chaperone (BiP-like). To acquire a thorough insight in the functional characterization of these identified secreted proteins, their tertiary structures were predicted. Considering the observed phenomenon wherein secreted proteins across various pathogenic kingdoms, sharing analogous functions in host organisms, exhibit similar folding patterns (Kotsaridis et al., 2023), alongside instances where virulence proteins manifest as bi-domain structures (Ma and Ma, 2016), a comprehensive comparative analysis was undertaken. This investigation encompassed not only the entire protein molecules but also their individual N'- and C'-terminal regions. As expected by the already annotation for the RSP27A protein, its N-terminus displayed structural similarity to the ubiquitin molecule (PDB:1XD3) with a root mean square deviation (RMSD) of 0.604, while the C-terminus aligned with the S27a of the 40S ribosomal subunit (PDB:6ZLW) with an RMSD of 0.592 (Fig. S7A, S8). Notably, the NL-SBP protein displayed structural similarity to Sxl protein of the Sxl-Unr translation regulatory complex (PDB:4QQB, (Hennig et al., 2014)), suggesting an RNA-binding in host activity with an RMSD value of 1.546 (Figs. 5B, S8). Next, the RPL27 protein was verified by high structural similarity to the 60S ribosomal protein L27-A (PDB: 7NAD) with an RMSD of 0.580 (Figs. S7B, S8). Interestingly, the PTF protein displayed structural similarity to CBRP1 (cellular retinol-binding protein 1) protein (PDB:6E6M), which was previously characterized to have lipid binding properties (Silvaroli et al.,
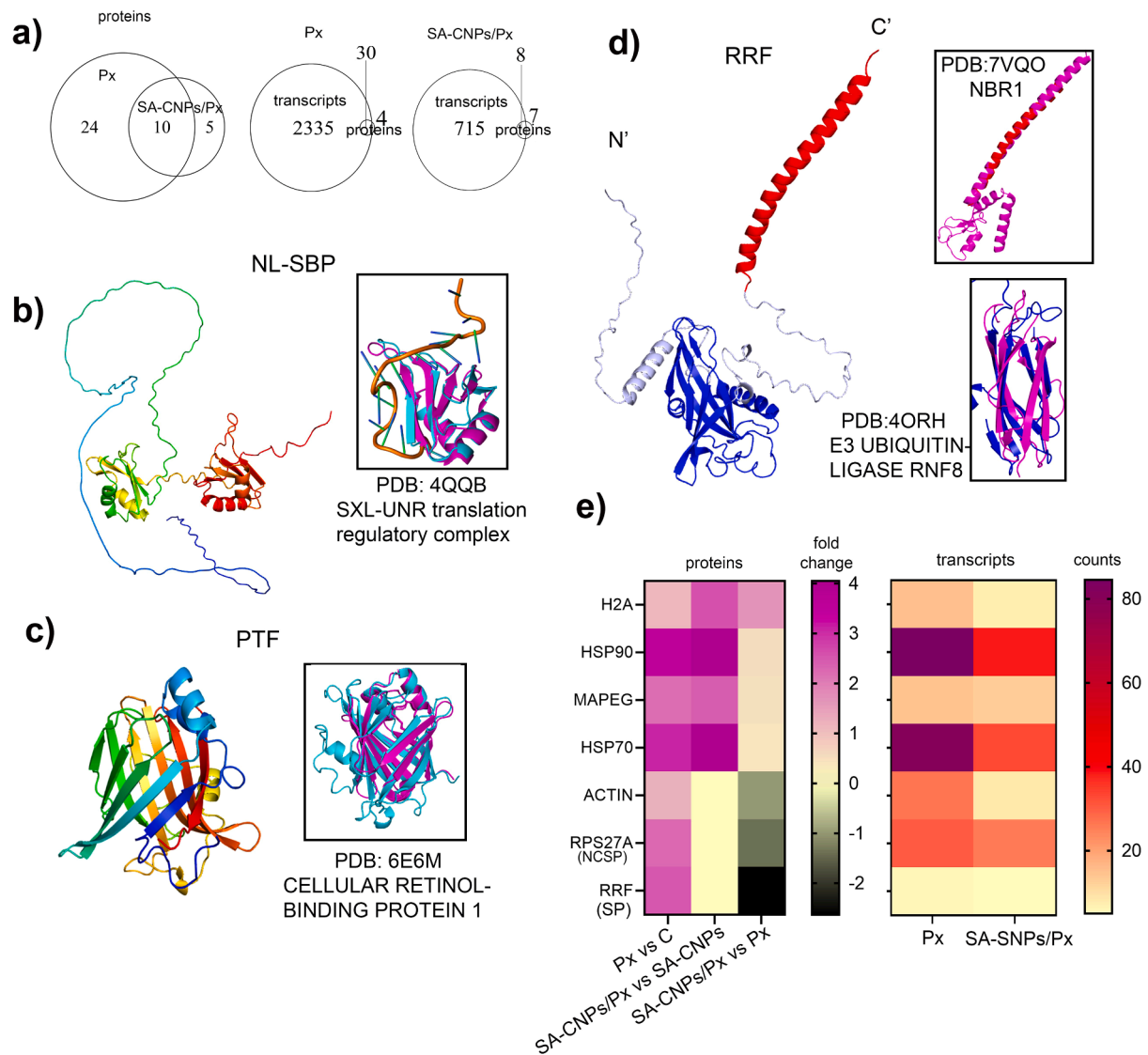
Fig. 5. Structure and expression of selected *P. xanthii* secreted proteins. **(a)** Overlaps of *P. xanthii* differentially expressed genes and proteins in the integrated transcriptomic and proteomic analysis. **(b)** Model of *P. xanthii* NL-SBP secreted protein (AlphaFold2). The rainbow color gradient represents the N-terminus in blue to C-terminus in red. In the box the functional motif is superimposed to experimentally determined domain structure shown in magenta. **(c)** Model of *P. xanthii* PTF secreted protein (AlphaFold2). The rainbow color gradient represents the N-terminus in blue to C-terminus in red. In the box the functional motif is superimposed to experimentally determined domain structure shown in magenta. **(d)** Model of *P. xanthii* RRF secreted protein (AlphaFold2). In the boxes the functional motifs are superimposed to experimentally determined domain structures shown in magenta. **(e)** Heatmaps showing *P. xanthii* matching differentially expressed genes and proteins in the integrated transcriptomic and proteomic analysis.

2019), with RMSD of 1.537 (Figs. 5C, S8). As for the RRF protein, distinct structural similarities emerged when analyzing the N'- and C'-terminal domains independently. The N-terminus exhibited structural resemblance to the autophagy receptor NBR1 protein domain (PDB:7VQO), with an RMSD value of 2.097, whereas the C-terminus was aligned with the E3 ubiquitin-protein ligase RNF8 (PDB:4ORH) with an RMSD of 0.718 (Figs. 5D, S8). Finally, the structural prediction of the BiP-like protein, an ER-resident molecular chaperone that plays key roles in stress responses (Hendershot, 2004), agreed with its previous functional characterization, since it showed structural similarity with the 78 kDa glucose-regulated protein (PDB:5E84, (Yang et al., 2015)) with a RMSD of 2.854 (Figs. S7C, S8). Overall, the investigation of the identified effectors revealed that the pathogen favors the UPS system to encounter plant's defense for effective virulence.

Next step was to evaluate how the plant's induced defense by SA-CNPs application, challenged the expression of these secreted proteins. First, we correlated the protein and transcript pools of the pathogen

between treatments, that allowed us to detect seven proteins that were quantified in all samples, indicating a trustworthy protein selection (Fig. 5E). Among all treatments, we noticed a similar expression of the histone H2A, that reflected a similar presence of *P. xanthii* conidia. On the other hand, the cytoskeletal ACTIN protein showed decreased expression after SA-CNPs application, that could correlate with the observed decreased number of conidia germination and growth (Fig. 1E). Interestingly, the two major molecular chaperones HSP90 and HSP70, were remarkably expressed in *P. xanthii* samples, and their expression was downregulated with 3- and 2.5 Log2fold-change (LogFC) in SA-CNPs/*P. xanthii* compared to *P. xanthii* protein samples (Fig. 5E). This difference speculates a key role of the molecular chaperones in pathogen's virulence that is challenged by host's induced defense. Similar expression pattern had the MAPEG protein, a membrane-associated protein in eicosanoid and glutathione metabolism, exhibiting cytoprotective role through glutathione S-transferase and peroxidase activities (Kammerscheit et al., 2019). Finally, as far as the secreted

proteins are concerned, only two were identified between all samples, the RPS27 and RRF, that are both related to the ubiquitin system (Catic and Ploegh, 2005). Their expression was substantially high in the *P. xanthii* samples, with 2.3- and 2.5 LogFC change respectively, reinforcing the conception that the pathogen utilizes the ubiquitination mechanism to induce host-specific protein degradation. Notably, both proteins were downregulated in the SA-CNPs/*P. xanthii* samples by −1.4- and −2.6 LogFC, respectively (Fig. 5E), which made us hypothesize that the defense mechanism of the host countered these pathogen effectors.

3.6. Arabidopsis induced defense by SA-CNPs involves endoplasmic reticulum-associated quality control

Thus, we speculated that since pathogen virulence exploited ubiquitination, plant defense could also engage a similar mechanism. To examine this, we classified the identified Arabidopsis proteins in our comparisons of interest according to their relationship with ubiquitin, the proteasome, and the ribosome. An overall differential expression analysis in the SA-CNPs vs Control comparison revealed 38 (30 up- and 8-downregulated) proteasome-specific, 238 (156 up- and 82-downregulated) ubiquitin-specific and 71 (58 up- and 13-dowregulated)
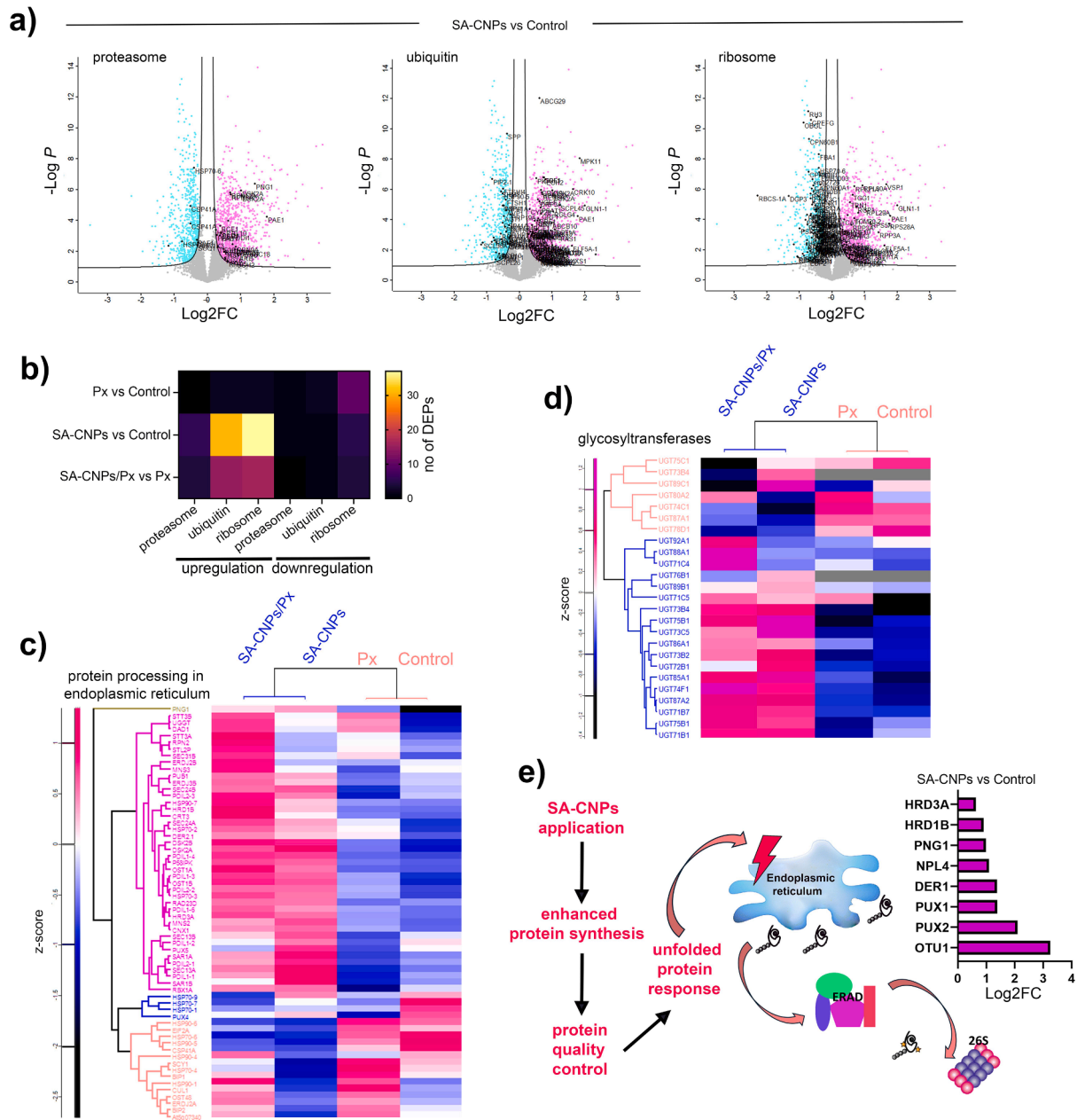
Fig. 6. SA-CNPs upregulate protein quality control in the ER. **(a)** Volcano plots showing the positive and negative differential expressed *A.thaliana* proteins SA-CNPs vs Control comparison. **(b)** Heatmap showing induced expression levels of *A. thaliana* proteins related to the proteasome, ubiquitin and the ribosome after SA-CNPs application. **(c)** Heatmap showing induced expression levels of *A. thaliana* proteins related to the KEGG 04,141 pathway of protein processing in endoplasmic reticulum after SA-CNPs application. **(d)** Heatmap showing induced expression levels of identified *A. thaliana* glycosyltransferases after SA-CNPs application. **(e)** Working model of upregulation of protein quality control in the endoplasmic reticulum after SA-CNPs application. SA-CNPs promote increased protein synthesis. Excess nascent proteins are subjected to quality control where the folding and glycosylation state of nascent proteins is inspected. Misfolded proteins promote stress response and ERAD aberrant substrate degradation. On the right side, expression levels of endoplasmic reticulum associated degradation (ERAD) proteins in the SA-CNPs versus Control comparison.

ribosome-specific significant DEPs (Fig. 6A, File S6). Limiting the detection in highly significant upregulated proteins, we detected 6 proteasomal, 31 ubiquitin-related and 37 ribosomal proteins, and when we compared this result to the *P. xanthii* vs Control comparison, the detected proteins in all classes were almost zero (Fig. 6B, File S6). In the SA-CNPs/*P. xanthii* vs *P. xanthii* comparison, even though the classified proteins were reduced than the SA-CNPs vs Control comparison, when compared to *P. xanthii* vs Control the difference was 4 in proteasomal, 13 in ubiquitin-related and 14 in ribosomal classes (Fig. 6B, File S6). Overall, these findings indicated that our speculation was reasonable and indeed, the induced defense of the plant involved increased expression of the degradation-related system.

In the downregulated protein groups, we noticed a completely reverse outcome. The expression of ribosomal-related proteins was predominantly affected, especially in the *P. xanthii* vs Control comparison where mainly components of the 60S and 40S ribosomal subunits were included in the 9 downregulated proteins (Fig. 6B, File S6). On the other hand, in the SA-CNPs vs Control and SA-CNPs/*P. xanthii* vs *P. xanthii* comparisons the downregulated ribosomal proteins were 6 and 4, respectively, with arbitrary localization or features (Fig. 6B, File S6).

An intriguing observation was the significant protein and pathway enrichment of components of the glycoprotein biosynthesis and secretion pathway that takes place at endoplasmic reticulum (ER) (Fig. 3D, 3E) and is directly linked to endoplasmic reticulum-associated degradation (ERAD) process and the proteasome (Xu and Ng, 2015). A comprehensive analysis of ER-related proteins, through the protein processing in endoplasmic reticulum pathway (KEGG 04,141), revealed essential upregulation of 43 (70 %) out of the 62 DEPs when SA-CNPs

are applied with and without pathogen inoculation (Fig. 6C). Among these were oligosaccharyltransferases (OSTs) that direct the ribosome to the ER membrane, UDP-glucose:glycoprotein glucosyltransferases (UGGT), and protein disulfide-isomerases (PDIs), that are components of the ERAD machinery (Xu and Ng, 2015), and COPII transport proteins such as SECRETION-ASSOCIATED RAS-RELATED PROTEIN 1 (SAR1) and SECRETORY PROTEINS (SECs) (Sato and Nakano, 2007) (Figs. 6C, S9). Moreover, when we searched specifically for UGTs, we found 25 proteins in our samples, and 18 of them (72 %) were upregulated after SA-CNPs application, with and without pathogen inoculation (Fig. 6D), demonstrating an induced glycosylation pathway. Collectively, functional analysis results demonstrated that SA-CNPs application enhanced the cascade of events leading from protein synthesis to glycosylation, to protein degradation. One could reasonably hypothesize that the integrated pathways of this cascade drive the production of increased number of defensive compounds and at the same time degrade misfolded proteins of this overactivated production or watch over for invasive proteins, a hypothesis that is reinforced by the upregulated expression of many components of the ERAD machinery (Fig. 6E).

3.7. The pathogen challenges host's protein production and quality control

The integration of our findings from both pathogen secreted proteins and the plant's responses after SA-CNPs application indicated the interplay with protein degradation mechanisms. To get a comprehensive understanding of the function of pathogen's effectors, we performed an in depth bioinformatic approach at the protein level. Alphafold2

Fig. 7. *P. xanthii* RPS27A secreted effector protein is implicated in protein quality control. **(a)** Models of the two functional domains of *P. xanthii* RPS27A secreted effector protein superimposed to experimentally determined domain structures of *A. thaliana* RPS27AA homologs (AlphaFold2). **(b)** PPI network of RPS27AA with identified proteins of the protein processing in endoplasmic reticulum pathway in *A.thaliana*. **(c)** PPI network of RPS27AA with identified downregulated ribosome-related proteins of the Px vs Control comparison in *A.thaliana*.

structural prediction showed that RPS27 shared identical structural homology to all six Arabidopsis 40S-eS31 ubiquitin-40S ribosomal protein variants (Figs. 7A, S10). Subsequently, we performed STRING analysis of the predominant Arabidopsis variant (RPS27AA) with proteins of the major groups that we identified as key players in this plant-pathogen interplay. Even though RPS27 did not interact with any protein of the highly induced pathways of the SA-CNPs versus Control comparison (Fig. 3D), we found highly significant interactions, with PPI enrichment *P-value*: < 5.09e-07, between RPS27AA and 12 (28 %) of the identified upregulated DEPs in the protein processing in endoplasmic reticulum pathway (Fig. 7B), indicating a direct link of RPS27AA with ER protein processing. Additionally, we examined ERAD-related proteins in the downregulated DEPs in the *P. xanthii* versus Control comparison to test if there is a connection between this effector and the pathways induced after SA-CNPs application. Interestingly, even though we did not detect interaction with any direct component of the pathway, there were a plethora of downregulated ribosome-related proteins, 18 (78 %) out of the 23, that interacted with RPS27AA with a PPI enrichment *P-value*: < 1.0e-16 (Fig. 7C). The excessive downregulation of the ribosomal proteins could be attributed to their immediate degradation due to incompetence of these proteins to accumulate in a functional ribosome (Ju et al., 2023), with the PPI network indicating a noteworthy involvement of the fungal effector in this outcome. Overall, our findings demonstrated that there is an alternation in the sequence of the protein degradation events that take place during pathogen virulence and host defense; the pathogen uses degradation to arrest the production of defense proteins, while the host uses degradation as part of the quality control due to excess protein production. The effectiveness of each event could lead to the prevalence of one against the other.

4. Discussion

In order for Pattern Recognition Receptors (PRRs) to synthesize and show a suited function against pathogen infection, they rely on N-glycosylation and ERQC system (Saijo et al., 2009). The ERQC system, consisting of the ERAD and the unfolded protein response (UPR), mediates and monitors the processing and folding of secretory proteins, important PM-resident proteins that are involved in responses to pathogen infection such as glycoproteins, hormone or immune receptors, and other proteins destined for transfer to the vacuole, or the apoplast (Wang et al., 2005). At the same time, ERQC identifies misfolded proteins, activates ER stress response by engaging UPR, glycosylates the substrates and transfers them to ERAD machinery (Araki and Nagata, 2011). Substrates for glycosylation can be from endogenous phytohormones, defensive and cell wall compounds and other secondary metabolites, to exogenous foreign compounds, such as toxins from pathogens (Bowles, 2005; Gharabli et al., 2023), indicating their immediate connection with plant responses to pathogens. Nevertheless, the intricate pathogens exploit effectors to hijack plant components of the ER stress pathway and manipulate them to gain compatibility and promote infection (Jing and Wang, 2020). There is growing evidence highlighting the ER stress response as a key target for pathogens, allowing them to control ER stress-mediated plant immunity. Various ER-associated proteins are influenced by infection of bacteria, oomycetes, necrotrophic or biotrophic fungi, but the effectors involved in these interactions are poorly known (Jing and Wang, 2020). Two identified effectors are the protein HopD1 from *Pseudomonas syringae* pv. *tomato* DC3000, that interacts with Arabidopsis ER resident protein NTM1-like 9 (Block et al., 2014), and the Pi03192 protein from *Phytophthora infestans* that directly interacts with two potato NAC062-related membrane anchored transcription factors linked to ER (McLellan et al., 2013; Yang et al., 2014). Here, our holistic approach showed that *P. xanthii* possess explicit tools to manipulate host ER stress pathway even from protein synthesis sensing. The *P. xanthii* RPS27 effector, which was highly expressed after artificial inoculation, is almost identical to the conserved ubiquitinated ribosomal eukaryotic protein 40S eS31 (RPS27AA in Arabidopsis), and

its function is considered a sophisticated mechanism to maintain the equilibrium between protein synthesis and degradation (Catic and Ploegh, 2005; Redman and Rechsteiner, 1989). Since *P. xanthii* is an obligate biotrophic pathogen relaying to its living host for growth, protein equilibrium is extremely vital because it reflects the ability of the pathogen to keep a balance between colonization and host preservation. The interaction of RPS27 homologue, RSP27AA, with a considerable number of ribosomal proteins, downregulated after pathogen inoculation, and with various components of the ERQC, upregulated after inducer application, highlights pathogen's ability in manipulating this network. Interestingly, a high number of ribosomal proteins was identified as secreted proteins in *P. xanthii*. Even though it could be considered a secretome contamination due to cell breakage (Rampitsch et al., 2013), there are evidence suggesting that ribosomal proteins could have broader functions and also contribute to virulence (Hurtado-Rios et al., 2022; Li et al., 2019), indicating the overall engagement of key protein production pathways in host-pathogen interactions. Additionally, our results are in agreement with current knowledge on how effector molecules degrade their targets by mimicking ubiquitination-related eukaryotic proteins (Langin et al., 2020).

On the other hand, defense inducers must be competent to prepare hosts against pathogen's mode of action, to be effective. PTI and ETI both depend on SA and induce SAR against a broad spectrum of (hemi-) biotrophic pathogens (Vlot et al., 2021), which includes the production of ROS and the expression and accumulation of PR proteins. Here, we showed that SA-CNPs can effectively induce the overall defense mechanism by significant ROS production and *PR1* expression upregulation, leading to noteworthy *P. xanthii* reduced germination. Moreover, induced defense was accompanied by promoted growth, as we observed by root growth measurements, that not only showed the positive effect of SA application on growth but could also be a desirable trait when the SA-CNPs formulation will be applied on a commercial crop. Nevertheless, the balance between defense and fitness should be carefully evaluated in order to achieve the optimum outcome (Huot et al., 2014).

For PR proteins to function properly, optimal coordination and regulation of the protein secretory machinery to ensure folding, modification, and transport is required and takes place in the ER, demonstrating the high dependence of PRs with ERQC (Poór et al., 2019). Additionally, other defense-related proteins depend on ERQC, such as LRR-RKs (Tintor and Saijo, 2014), the BARLEY POWDERY RESISTANCE O (MLO) protein (Muller et al., 2005), and cell wall $\beta-1,3/\beta-1,6$-glucans (Chaliha et al., 2018). SA-CNPs application in this work, upregulated the expression of LRR-RKs proteins, resistance-associated genes, where among these were three powdery mildew resistance proteins and endo-1,3-beta-glucosidases, that hydrolyze 1,3-beta-D-glucosidic linkages in 1,3-beta-D-glucans (Table S7), reinforcing the inducible interaction of ERQC with defense components.

Client proteins that fail to fold or assemble correctly in ERQC, are transported into cytoplasm for degradation by ERAD, the ATP-dependent ubiquitin–proteasome system (UPS) (Araki and Nagata, 2011). More interestingly, UPS is involved in the controlled turnover of key regulatory proteins of plant defense. The well-known LRR-RKs in Arabidopsis, FLAGELLIN-SENSITIVE 2 (FLS2) and CHITIN ELICITOR RECEPTOR KINASE 1 (CERK1), which are phosphorylated for signal transduction, undergo UPS-associated turnover, and moreover, various intracellular immune receptors, such as (NLR) proteins, integrate with the UPS system (Langin et al., 2023). Additionally, as the biotrophic pathogens are concerned, the key transcriptional regulator of the SA-mediated defense response, NON-EXPRESSOR OF PR GENES 1 (NPR1) protein, is ubiquitinated and targeted for proteasomal degradation in relation to SA accumulation levels (Fu et al., 2012). This evidence is in accordance with our observations on the combined modifications in expression of both defense-related and a plethora of ERAD proteins after SA-CNPs application in Arabidopsis. Altogether, these findings indicate how the ERQC acts as a central regulator of

immune signaling pathways and that proper execution of defense responses relies on the induction of ERQC genes.

In previous works, we showed that a plant-derived defense inducer positively influenced *Cucurbita pepo* plants against *P. xanthii* through the SA defense pathway and that components of the plant plasma membrane are key players in the upstream activation of this pathway (Margaritopoulou et al., 2024, 2020). In this study, we demonstrated that SA can be effectively transferred inside the plant by this new generation of biodegradable nanoparticles, show similar defense response reactions in *A. thaliana* against *P. xanthii* and most importantly we elucidated the downstream defense responses that lead to pathogen resistance.

5. Conclusion

The recent years, it is becoming clear that the ERQC is a major immune hub, involved in all stages of plant defenses against various kinds of pathogens across most plant species. However, this interconnection is complex and versatile generating a flexible response of plant defense machinery against pathogen infection. Our evidence demonstrates an emerging field of a highly potential control strategy against biotrophic pathogens by the form of activating ER stress-mediated plant immunity. The engagement of the RPS27A effector in fungal virulence and the protein processing in endoplasmic reticulum (ER)- and glycosyltransferase-related proteins in plant induced defense response, that are all constituents of ERQC, shows that this conserved quality control system of the cell underlies in plant pathogen interactions. The integration of both partners in this pathway offers valuable insights into potential antagonistic fungal resources targeting biotrophic pathogens. Further exploration and development of resources, such as eco-friendly biodegradable nanoparticles, that modulate this pathway will contribute to novel disease management strategies against biotrophic pathogens, enriching our understanding of these resources.

CRediT authorship contribution statement

Theoni Margaritopoulou: Writing – review & editing, Writing – original draft, Supervision, Software, Methodology, Investigation, Data curation, Conceptualization. **Konstantinos Kotsaridis:** Writing – review & editing, Software, Data curation. **Martina Samiotaki:** Writing – review & editing, Software, Methodology, Data curation. **Spyridon Nastos:** Investigation. **Marinos Maratos:** Investigation. **Ieronymos Zoidakis:** Writing – review & editing, Investigation, Formal analysis. **Despoina Tsiriva:** Methodology, Investigation. **Stergios Pispas:** Methodology, Investigation. **Emilia Markellou:** Writing – review & editing, Supervision, Investigation, Funding acquisition, Data curation, Conceptualization.

Declaration of competing interest

The authors declare the following financial interests/personal relationships which may be considered as potential competing interests:

Despoina Tsiriva has a European patent application that describes the formulation of chitosan-based nanoparticles for large-scale commercial production. All other authors have no conflicts to declare.

Acknowledgments

Supplementary materials

Supplementary material associated with this article can be found, in the online version, at doi:10.1016/j.stress.2024.100693.

Data availability

Data will be made available on request.

References

Ahmed, H., Howton, T., Sun, Y., Weinberger, N., Belkhadir, Y., Mukhtar, M.S., 2018. Network biology discovers pathogen contact points in host protein-protein interactomes. Nat. Commun. 9, 2312.

An, J., Kim, S.H., Bahk, S., Le Anh Pham, M., Park, J., Ramadany, Z., Lee, J., Hong, J.C., Chung, W.S., 2023. Quercetin induces pathogen resistance through the increase of salicylic acid biosynthesis in Arabidopsis. Plant Signal. Behav. 18, 2270835.

Anders, S., 2010. Analysing RNA-Seq data with the DESeq package. Mol. Biol. 43, 1–17.

Anders, S., Pyl, P.T., Huber, W., 2015. HTSeq—A Python framework to work with high-throughput sequencing data. Bioinformatics 31, 166–169.

Araki, K., Nagata, K., 2011. Protein folding and quality control in the ER. Cold Spring Harb. Perspect. Biol. 3, a007526.

Bashir, S.M., Ahmed Rather, G., Patrício, A., Haq, Z., Sheikh, A.A., Shah, M.Z.u.H., Singh, H., Khan, A.A., Imtiyaz, S., Ahmad, S.B., 2022. Chitosan nanoparticles: a versatile platform for biomedical applications. Materials 15, 6521 (Basel).

Beckers, G.J., Jaskiewicz, M., Liu, Y., Underwood, W.R., He, S.Y., Zhang, S., Conrath, U., 2009. Mitogen-activated protein kinases 3 and 6 are required for full priming of stress responses in Arabidopsis thaliana. Plant Cell 21, 944–953.

Berman, H., Henrick, K., Nakamura, H., 2003. Announcing the worldwide protein data bank. Nat. Struct. Mol. Biol. 10, 980.

Bertini, L., Proietti, S., Aleandri, M.P., Mondello, F., Sandini, S., Caporale, C., Caruso, C., 2012. Modular structure of HEL protein from Arabidopsis reveals new potential functions for PR-4 proteins. Biol. Chem. 393, 1533–1546.

Block, A., Toruño, T.Y., Elowsky, C.G., Zhang, C., Steinbrenner, J., Beynon, J., Alfano, J. R., 2014. The P seudomonas syringae type III effector H op D 1 suppresses effector-triggered immunity, localizes to the endoplasmic reticulum, and targets the A rabidopsis transcription factor NTL 9. New Phytol. 201, 1358–1370.

Bowles, D., 2005. Glycosyltransferases of lipophilic small molecules. Curr. Opin. Plant Biol. 8, 254–263.

Bray, N.L., Pimentel, H., Melsted, P., Pachter, L., 2016. Near-optimal probabilistic RNA-seq quantification. Nat. Biotechnol. 34, 525–527.

Bremmer, J., Gonzalez-Martinez, A., Jongeneel, R., Huiting, H., Stokkers, R., Ruijs, M., 2021. Impact Assessment of EC 2030 Green Deal Targets for Sustainable Crop Production. Wageningen Economic Research.

Catic, A., Ploegh, H.L., 2005. Ubiquitin–conserved protein or selfish gene? Trends Biochem. Sci. 30, 600–604.

Chaliha, C., Rugen, M.D., Field, R.A., Kalita, E., 2018. Glycans as modulators of plant defense against filamentous pathogens. Front. Plant Sci. 9, 363767.

Chu, E.W., and Karr, J.R. (2017). Environmental impact: concept, consequences, measurement. Reference module in life sciences.

Committee, E.S., 2021. Guidance on risk assessment of nanomaterials to be applied in the food and feed chain: human and animal health. EFSA J. 19, e06768.

DeFalco, T.A., Zipfel, C., 2021. Molecular mechanisms of early plant pattern-triggered immune signaling. Mol. Cell 81, 3449–3467.

Demichev, V., Messner, C.B., Vernardis, S.I., Lilley, K.S., Ralser, M., 2020. DIA-NN: neural networks and interference correction enable deep proteome coverage in high throughput. Nat. Methods 17, 41–44.

Dobin, A., Davis, C.A., Schlesinger, F., Drenkow, J., Zaleski, C., Jha, S., Batut, P., Chaisson, M., Gingeras, T.R., 2013. STAR: ultrafast universal RNA-seq aligner. Bioinformatics 29, 15–21.

Dodds, P.N., Rathjen, J.P., 2010. Plant immunity: towards an integrated view of plant–pathogen interactions. Nat. Rev. Genet. 11, 539–548.

Falk, A., Feys, B.J., Frost, L.N., Jones, J.D., Daniels, M.J., Parker, J.E., 1999. EDS1, an essential component of R gene-mediated disease resistance in Arabidopsis has homology to eukaryotic lipases. Proc. Natl. Acad. Sci. 96, 3292–3297.

Faqir, Y., Ma, J., Chai, Y., 2021. Chitosan in modern agriculture production. Plant Soil Environ. 67, 679–699.

Fu, Z.Q., Yan, S., Saleh, A., Wang, W., Ruble, J., Oka, N., Mohan, R., Spoel, S.H., Tada, Y., Zheng, N., 2012. NPR3 and NPR4 are receptors for the immune signal salicylic acid in plants. Nature 486, 228–232.

Gaffney, T., Friedrich, L., Vernooij, B., Negrotto, D., Nye, G., Uknes, S., Ward, E., Kessmann, H., Ryals, J., 1993. Requirement of salicylic acid for the induction of systemic acquired resistance. Science 261, 754–756 (1979).

Gan, P.H., Dodds, P.N., Hardham, A.R., 2011. Plant infection by biotrophic fungal and oomycete pathogens. Signaling and Communication in Plant Symbiosis. Springer, pp. 183–212.

Gharabli, H., Della Gala, V., Welner, D.H, 2023. The function of UDP-glycosyltransferases in plants and their possible use in crop protection. Biotechnol. Adv., 108182

Gullner, G., Komives, T., Király, L., Schröder, P., 2018. Glutathione S-transferase enzymes in plant-pathogen interactions. Front. Plant Sci. 9, 427485.

Hendershot, L.M., 2004. The ER chaperone BiP is a master regulator of ER function. Mount Sinai J. Med. 71.

Hennig, J., Militti, C., Popowicz, G.M., Wang, I., Sonntag, M., Geerlof, A., Gabel, F., Gebauer, F., Sattler, M., 2014. Structural basis for the assembly of the Sxl–Unr translation regulatory complex. Nature 515, 287–290.

Holm, L., 2020. Using Dali for protein structure comparison. Struct. Bioinform. Methods Protoc. 29–42.

Hughes, C.S., Moggridge, S., Müller, T., Sorensen, P.H., Morin, G.B., Krijgsveld, J., 2019. Single-pot, solid-phase-enhanced sample preparation for proteomics experiments. Nat. Protoc. 14, 68–85.

Huot, B., Yao, J., Montgomery, B.L., He, S.Y., 2014. Growth–defense tradeoffs in plants: a balancing act to optimize fitness. Mol. Plant 7, 1267–1287.

Hurtado-Rios, J.J., Carrasco-Navarro, U., Almanza-Pérez, J.C., Ponce-Alquicira, E., 2022. Ribosomes: the new role of ribosomal proteins as natural antimicrobials. Int. J. Mol. Sci. 23, 9123.

Ingle, P.U., Shende, S.S., Shingote, P.R., Mishra, S.S., Sarda, V., Wasule, D.L., Rajput, V.D., Minkina, T., Rai, M., Sushkova, S., 2022. Chitosan Nanoparticles (ChNPs): A versatile Growth Promoter in Modern Agricultural Production. Heliyon.

Jaswal, R., Kiran, K., Rajarammohan, S., Dubey, H., Singh, P.K., Sharma, Y., Deshmukh, R., Sonah, H., Gupta, N., Sharma, T., 2020. Effector biology of biotrophic plant fungal pathogens: current advances and future prospects. Microbiol. Res. 241, 126567.

Jefferson, R.A., Kavanagh, T.A., Bevan, M.W., 1987. GUS fusions: beta-glucuronidase as a sensitive and versatile gene fusion marker in higher plants. EMBO J. 6, 3901–3907.

Jing, M., Wang, Y., 2020. Plant pathogens utilize effectors to hijack the host endoplasmic reticulum as part of their infection strategy. Engineering 6, 500–504.

Ju, D., Li, L., Xie, Y., 2023. Homeostatic regulation of ribosomal proteins by ubiquitin-independent cotranslational degradation. Proc. Natl. Acad. Sci. 120, e2306152120.

Jumper, J., Evans, R., Pritzel, A., Green, T., Figurnov, M., Ronneberger, O., Tunyasuvunakool, K., Bates, R., Žídek, A., Potapenko, A., 2021. Highly accurate protein structure prediction with AlphaFold. Nature 596, 583–589.

Kammerscheit, X., Chauvat, F., Cassier-Chauvat, C., 2019. From cyanobacteria to human, MAPEG-type glutathione-S-transferases operate in cell tolerance to heat, cold, and lipid peroxidation. Front. Microbiol. 10, 491407.

Kemen, A.C., Agler, M.T., Kemen, E., 2015. Host–microbe and microbe–microbe interactions in the evolution of obligate plant parasitism. New Phytol. 206, 1207–1228.

Kim, S., Subramaniyam, S., Jung, M., Oh, E.A., Kim, T.H., Kim, J.G., 2021. Genome resource of Podosphaera xanthii, the host-specific fungal pathogen that causes cucurbit powdery mildew. Mol. Plant-Microbe Interact. 34, 457–459.

Kotsaridis, K., Michalopoulou, V.A., Tsakiri, D., Kotsifaki, D., Kefala, A., Kountourakis, N., Celie, P.H., Kokkinidis, M., Sarris, P.F., 2023. The functional and structural characterization of Xanthomonas campestris pv. campestris core effector XopP revealed a new kinase activity. Plant J. 116, 100–111.

Langin, G., Gouguet, P., Üstün, S., 2020. Microbial effector proteins–a journey through the proteolytic landscape. Trends Microbiol. 28, 523–535.

Langin, G., González-Fuente, M., Üstün, S., 2023. The plant ubiquitin–proteasome system as a target for microbial manipulation. Annu. Rev. Phytopathol. 61, 351–375.

Lee, S., Kim, S.M., Lee, R.T., 2013. Thioredoxin and thioredoxin target proteins: from molecular mechanisms to functional significance. Antioxid. Redox Signal. 18, 1165–1207.

Li, A., Sun, X., Liu, L., 2022. Action of salicylic acid on plant growth. Front. Plant Sci. 13, 878076.

Li, T., Wu, Y., Wang, Y., Gao, H., Gupta, V.K., Duan, X., Qu, H., Jiang, Y., 2019. Secretome profiling reveals virulence-associated proteins of Fusarium proliferatum during interaction with banana fruit. Biomolecules 9, 246.

Liu, X., Ma, Z., Tran, T.M., Rautengarten, C., Cheng, Y., Yang, L., Ebert, B., Persson, S., Miao, Y., 2024. Balanced callose and cellulose biosynthesis in Arabidopsis quorum-sensing signaling and pattern-triggered immunity. Plant Physiol. 194, 137–152.

Ma, K.W., Ma, W., 2016. YopJ family effectors promote bacterial infection through a unique acetyltransferase activity. Microbiol. Mol. Biol. Rev. 80, 1011–1027.

Margaritopoulou, T., Baira, E., Anagnostopoulos, C., Vichou, K.E., Markellou, E., 2024. Phospholipid production and signaling by a plant defense inducer against Podosphaera xanthii is genotype-dependent. Hortic. Res. 11, uhae190.

Margaritopoulou, T., Toufexi, E., Kizis, D., Balayiannis, G., Anagnostopoulos, C., Theocharis, A., Rempelos, L., Troyanos, Y., Leifert, C., Markellou, E., 2020. Reynoutria sachalinensis extract elicits SA-dependent defense responses in courgette genotypes against powdery mildew caused by Podosphaera xanthii. Sci. Rep. 10, 3354.

Margaritopoulou, T., Kizis, D., Kotopoulis, D., Papadakis, I.E., Anagnostopoulos, C., Baira, E., Termentzi, A., Vichou, A.E., Leifert, C., Markellou, E., 2022. Enriched H3K4me3 marks at Pm-0 resistance-related genes prime courgette against Podosphaera xanthii. Plant Physiol. 188, 576–592.

McLellan, H., Boevink, P.C., Armstrong, M.R., Pritchard, L., Gomez, S., Morales, J., Whisson, S.C., Beynon, J.L., Birch, P.R., 2013. An RxLR effector from Phytophthora infestans prevents re-localisation of two plant NAC transcription factors from the endoplasmic reticulum to the nucleus. PLoS Pathog. 9, e1003670.

Muller, J., Piffanelli, P., Devoto, A., Miklis, M., Elliott, C., Ortmann, B., Schulze-Lefert, P., Panstruga, R., 2005. Conserved ERAD-like quality control of a plant polytopic membrane protein. Plant Cell 17, 149–163.

Nogly, P., Gushchin, I., Remeeva, A., Esteves, A.M., Borges, N., Ma, P., Ishchenko, A., Grudinin, S., Round, E., Moraes, I., 2014. X-ray structure of a CDP-alcohol phosphatidyltransferase membrane enzyme and insights into its catalytic mechanism. Nat. Commun. 5, 4169.

Polyakov, V., Bauer, T., Butova, V., Minkina, T., Rajput, V.D., 2023. Nanoparticles-based delivery systems for salicylic acid as plant growth stimulator and stress alleviation. Plants 12, 1637.

Poór, P., Czékus, Z., Tari, I., Ördög, A., 2019. The multifaceted roles of plant hormone salicylic acid in endoplasmic reticulum stress and unfolded protein response. Int. J. Mol. Sci. 20, 5842.

Pruitt, R.N., Locci, F., Wanke, F., Zhang, L., Saile, S.C., Joe, A., Karelina, D., Hua, C., Fröhlich, K., Wan, W.L., 2021. The EDS1–PAD4–ADR1 node mediates Arabidopsis pattern-triggered immunity. Nature 598, 495–499.

Rampitsch, C., Day, J., Subramaniam, R., Walkowiak, S., 2013. Comparative secretome analysis of F usarium graminearum and two of its non-pathogenic mutants upon deoxynivalenol induction in vitro. Proteomics 13, 1913–1921.

Redman, K.L., Rechsteiner, M., 1989. Identification of the long ubiquitin extension as ribosomal protein S27a. Nature 338, 438–440.

Reglinski, T., Havis, N., Rees, H.J., de Jong, H., 2023. The practical role of induced resistance for crop protection. Phytopathology® 113, 719–731.

Saijo, Y., Tintor, N., Lu, X., Rauf, P., Pajerowska-Mukhtar, K., Häweker, H., Dong, X., Robatzek, S., Schulze-Lefert, P., 2009. Receptor quality control in the endoplasmic reticulum for plant innate immunity. EMBO J. 28, 3439–3449.

Sato, K., Nakano, A., 2007. Mechanisms of COPII vesicle formation and protein sorting. FEBS Lett. 581, 2076–2082.

Schrödinger, L., and DeLano, W. (2020). PyMOL.

Sembada, A.A., Lenggoro, I.W., 2024. Transport of nanoparticles into plants and their detection methods. Nanomaterials 14, 131.

Shannon, P., Markiel, A., Ozier, O., Baliga, N.S., Wang, J.T., Ramage, D., Amin, N., Schwikowski, B., Ideker, T., 2003. Cytoscape: a software environment for integrated models of biomolecular interaction networks. Genome Res. 13, 2498–2504.

Silvaroli, J.A., Widjaja-Adhi, M.A.K., Trischman, T., Chelstowska, S., Horwitz, S., Banerjee, S., Kiser, P.D., Blaner, W.S., Golczak, M., 2019. Abnormal cannabidiol modulates vitamin A metabolism by acting as a competitive inhibitor of CRBP1. ACS Chem. Biol. 14, 434–448.

Stael, S., Kmiecik, P., Willems, P., Van Der Kelen, K., Coll, N.S., Teige, M., Van Breusegem, F., 2015. Plant innate immunity–sunny side up? Trends Plant Sci. 20, 3–11.

Survila, M., Davidsson, P.R., Pennanen, V., Kariola, T., Broberg, M., Sipari, N., Heino, P., Palva, E.T., 2016. Peroxidase-generated apoplastic ROS impair cuticle integrity and contribute to DAMP-elicited defenses. Front. Plant Sci. 7, 1945.

Tian, H., Wu, Z., Chen, S., Ao, K., Huang, W., Yaghmaiean, H., Sun, T., Xu, F., Zhang, Y., Wang, S., 2021. Activation of TIR signalling boosts pattern-triggered immunity. Nature 598, 500–503.

Tintor, N., Saijo, Y., 2014. ER-mediated control for abundance, quality, and signaling of transmembrane immune receptors in plants. Front. Plant Sci. 5, 81946.

Tyanova, S., Temu, T., Sinitcyn, P., Carlson, A., Hein, M.Y., Geiger, T., Mann, M., Cox, J., 2016. The Perseus computational platform for comprehensive analysis of (prote) omics data. Nat. Methods 13, 731–740.

Vaghela, B., Vashi, R., Rajput, K., Joshi, R., 2022. Plant chitinases and their role in plant defense: a comprehensive review. Enzyme Microb. Technol. 159, 110055.

Van Loon, L.C., Van Strien, E., 1999. The families of pathogenesis-associated proteins, their activities, and comparative analysis of PR-1 type proteins. Physiol. Mol. Plant Pathol. 55, 85–97.

Vlot, A.C., Sales, J.H., Lenk, M., Bauer, K., Brambilla, A., Sommer, A., Chen, Y., Wenig, M., Nayem, S., 2021. Systemic propagation of immunity in plants. New Phytol. 229, 1234–1250.

Wang, D., Weaver, N.D., Kesarwani, M., Dong, X., 2005. Induction of protein secretory pathway is required for systemic acquired resistance. Science 308, 1036–1040 (1979).

Wang, Z., Du, Y., Li, S., Xu, X., Chen, X., 2023. A complete genome sequence of Podosphaera xanthii isolate YZU573, the causal agent of powdery mildew isolated from cucumber in China. Pathogens 12, 561.

Xu, C., Ng, D.T., 2015. Glycosylation-directed quality control of protein folding. Nat. Rev. Mol. Cell Biol. 16, 742–752.

Yang, J., Nune, M., Zong, Y., Zhou, L., Liu, Q., 2015. Close and allosteric opening of the polypeptide-binding site in a human Hsp70 chaperone BiP. Structure 23, 2191–2203.

Yang, Z.T., Lu, S.J., Wang, M.J., Bi, D.L., Sun, L., Zhou, S.F., Song, Z.T., Liu, J.X., 2014. A plasma membrane-tethered transcription factor, NAC 062/ANAC 062/NTL 6, mediates the unfolded protein response in Arabidopsis. Plant J. 79, 1033–1043.

Yuan, M., Ngou, B.P.M., Ding, P., Xin, X.F., 2021. PTI-ETI crosstalk: an integrative view of plant immunity. Curr. Opin. Plant Biol. 62, 102030.